Feast and Famine: Regulation of Black Hole Growth in Low Redshift Galaxies

Guinevere Kauffmann[1] and Timothy M. Heckman[2],

[1] *Max-Planck Institut für Astrophysik, D-85748 Garching, Germany*
[2] *Center for Astrophysical Sciences, Department of Physics and Astronomy, Johns Hopkins University, Baltimore, MD 21218*

Abstract

We analyze the observed distribution of Eddington ratios (L/L_{Edd}) as a function of supermassive black hole mass for a large sample of nearby galaxies drawn from the Sloan Digital Sky Survey. We demonstrate that there are two distinct regimes of black hole growth in nearby galaxies. The first is associated with galaxies with significant star formation ($M_*/SFR \sim$ a Hubble time) in their central kiloparsec regions, and is characterized by a broad log-normal distribution of accretion rates peaked at a few percent of the Eddington limit. In this regime, the Eddington ratio distribution is independent of the mass of the black hole and shows little dependence on the central stellar population of the galaxy. The second regime is associated with galaxies with old central stellar populations ($M_*/SFR >>$ a Hubble time), and is characterized by a power-law distribution function of Eddington ratios. In this regime, the time-averaged mass accretion rate onto black holes is proportional to the mass of stars in the galaxy bulge, with a constant of proportionality that depends on the mean stellar age of the stars. This result is once again independent of black hole mass. We show that both the slope of the power-law and the decrease in the accretion rate onto black holes in old galaxies are consistent with population synthesis model predictions of the decline in stellar mass loss rates as a function of mean stellar age. Our results lead to a very simple picture of black hole growth in the local Universe. If the supply of cold gas in a galaxy bulge is plentiful, the black hole regulates its own growth at a rate that does not further depend on the properties of the interstellar medium. Once the gas runs out, black hole growth is regulated by the rate at which evolved stars lose their mass.

Keywords: galaxies:active – galaxies:bulges – galaxies:evolution – galaxies:nuclei: – galaxies:stellar content

1 Introduction

Large surveys of active galactic nuclei (AGN) teach us a great deal about the growth of supermassive black holes in galaxies as a function of cosmic time. By comparing quasar counts at different redshifts to the mass and number densities of black holes in the present-day Universe, one can derive constraints on the radiative efficiencies and lifetimes of these systems (e.g. Soltan 1982; Yu & Tremaine 2002). Additional constraints on quasar lifetimes also come from the measured clustering amplitude of these objects (e.g. Martini & Weinberg 2001; Shen et al 2007; Shankar et al 2008). There is now general consensus that optically luminous quasars are radiating close to their Eddington limit (Kollmeier et al. 2006), have short($\sim 10^7$ yr) lifetimes, and in total account for a sizeable fraction of the total mass density in black holes at the present day (Yu & Tremaine 2002).

By number, however, quasars only account for a small fraction of the total AGN population. Studies of complete samples of AGN in the local Universe (e.g. Heckman 1980, Ho, Filippenko & Sargent 1997; Kauffmann et al 2003b; Hao et al 2005) have taught us that the AGN fraction in massive galaxies with $> 10^{10.5} M_{\odot}$ galaxies is very high (> 50 %) and that AGN span a large range in Eddington ratios (Heckman et al 2004; Ho 2008). In lower-luminosity and optically-obscured (Type 2) AGN, the active nucleus does not outshine the underlying host galaxy, so one can carry out joint analyses of the accretion rate as a function of the physical properties of the host, and attempt to figure out which processes may be involved in triggering accretion onto the central black hole. Such studies have demonstrated that black hole growth is generally more rapid in low-redshift galaxies with younger stellar populations (Kauffmann et al. 2003b; Cid Fernandes et al. 2004). Moreover, the average ratio between the mass of stars forming in the bulge and the mass being accreted by the black hole is ~ 1000 (Heckman et al. 2004), which is very similar to the ratio between bulge mass and black hole mass in present-day inactive elliptical galaxies and bulges (Marconi & Hunt 2003; Haring & Rix 2004). This provides important confirmation that bulge formation and black hole growth are indeed still connected today, at least in an average sense.

It is important to try and pinpoint which *physical mechanisms* are responsible for the link between black hole growth and star formation in the host galaxy. One idea that has gained considerable popularity in recent years is that gravitational torques that arise during galaxy-galaxy mergers or interactions drive gas into the nuclear regions of galaxies, where it is able to fuel a central starburst and also accrete onto the black hole (e.g. Sanders et al 1988; Kauffmann & Haehnelt 2000; Granato et al 2004; Croton et al 2006). It is possible to model these processes in considerable detail using numerical simulations (Barnes & Hernquist 1991,1996; Mihos & Hernquist 1996). In more recent simulations (Di Matteo et al 2005; Springel et al 2005), some of the energy of the accreting black holes couples to the surrounding gas, and black hole growth eventually shuts down when the feedback energy is sufficient to unbind the reservoir of gas. Hopkins et al (2005 a,b) have used these simulations to derive physically-motivated light curves for AGN as a function of time in a large suite of simulations of merging galaxies, and to derive from this the luminosity-dependent lifetime distribution of AGN, under the assumption that they are triggered by mergers. In a more recent paper, Hopkins & Hernquist (2008) show how observed Eddington ratio distributions for complete samples of AGN are able to place strong constraints on different models for how black holes are fueled, and find that the available data agrees with the merger model predictions.

Observationally, there is still considerable debate as to whether any link exists between mergers/interactions and accretion onto the black hole. The best current constraints again come from studies of large samples of low redshift AGN. Recent clustering studies demonstrate that the star formation rates in galaxies are strongly enhanced if they have close neighbors, but that there is no similar enhancement in nuclear activity (Li et al 2006, 2008). Similarly, Reichard et al (2008) have used the lopsidedness in the stellar light distribution of SDSS galaxies as a signpost of interactions

and mergers. They find a strong link between lopsidedness and star formation, but they also demonstrate that if AGN and non-AGN samples are matched to have the same stellar masses, structural properties and central stellar populations, there is no difference in the lopsidedness of the light distribution between the active and non-active galaxies. If mergers and interactions are not instrumental in fueling accretion onto the central black holes of nearby galaxies, then other mechanisms such as bar-driven instabilities (Shlosman, Frank & Begelman 1989; Garcia-Burillo et al 2005) or stellar mass loss in galactic bulges (Mathews & Baker 1971; Norman & Scoville 1988; Ciotti & Ostriker 1997,2007) may play a more important role in explaining observed connection between AGN activity and recent star formation in the bulge.

In this paper, we re-examine the relationship between the accretion rates onto black holes and star formation in their host galaxies. Samples of nearby AGN are now sufficiently large to enable us to study not only the average relation between black hole accretion and star formation, but also how the *distribution functions* of black hole accretion rates vary as a function of black hole mass, and how the shapes of these distribution functions are modulated as the physical conditions and stellar populations in the galaxy change. As we will show, the full distribution function of accretion rates does indeed contain new information, and allows us to identify two clearly distinct "modes" of black hole growth in the local Universe. One mode is connected with galaxies with an ample supply of cold gas, and the other is connected with galaxies with aging and passively evolving stellar populations, where cold gas is presumably in much shorter supply. We then speculate on the physical origin of the two modes in view of recent ideas about how black holes are formed and fueled.

2 Methodology

We are interested in this paper in calculating the distribution of the Eddington ratio (L_{bol}/L_{Edd}) as a function of the key properties of the galaxies and their black holes. Our sample is drawn from the Data Release 4 (DR4) of the Sloan Digital Sky Survey (York et al 2000; Adelman-McCarthey et al 2006). The spectroscopic quantities we refer to are available for public download at http://www.mpa-garching.mpg.de/SDSS/DR4/.

To examine the dependence of the distribution of the Eddington ratio on the star formation history of the galaxy, we will use the amplitude of the 4000 Å break (as measured in the SDSS spectra with the $D_n(4000)$ index introduced by Balogh et al. (1999)). As discussed by Kauffmann et al. (2003a), the value of $D_n(4000)$ increases monotonically as the luminosity-weighted mean age of the stellar population increases. This dependence was quantified empirically by Brinchmann et al. (2004) who used SDSS spectroscopic measurements of the luminosity of the extinction-corrected Hα emission-line in star forming galaxies to relate the star formation rate per unit stellar mass (SFR/M_*) to the value of $D_n(4000)$. Obviously these two quantities are only related in an average sense, because the Brinchmann et al measurements were derived using emission line fluxes, which come from stars with ages less than 10^7 years, whereas $D_n(4000)$ is sensitive to young stars with a much broader range in age (> 1 Gyr).

We will estimate the black hole mass using the stellar velocity dispersions measured from the SDSS spectra and the formula given in Tremaine et al (2002). To estimate the bolometric luminosity, we will use the luminosity of the [OIII]λ5007 emission-line. The rationale for this is discussed in some detail in Heckman et al. (2004), but the primary reasons are that the [OIII] emission-line is one of the strongest lines in SDSS spectra and that it suffers substantially less contamination by emission from star forming regions than other strong lines. We will return to this latter point below. In Heckman et al (2004) the [OIII] line luminosities were not corrected for extinction by dust. This was because we used calibrations between [OIII] line luminosity and bolometric luminosity for Type 1 Seyferts and low-z quasars to calibrate L[OIII]/M_{BH} in units of the Eddington luminosity. Balmer

decrement measurements for the narrow emission-lines are not generally available for the Type 1 Seyferts and quasars. We thus decided to work with uncorrected line luminosities. The Heckman et al (2004) paper was mainly concerned with *average* accretion rates. In this paper we will be determining the distributions of the accretion rate as a function of the age of the stellar population. Dust corrections can be substantial, and will be systematically higher for AGN in galaxies with higher levels of ongoing star formation (Kauffmann et al. 2003b). Thus in this paper we will apply dust extinction corrections using the measured Balmer decrements in conjunction with a standard extinction law (following the procedure outlined in Kewley et al (2002).

While we will present our results in terms of the luminosity ratio log L[OIII]/M$_{BH}$ (hereafter, the Eddington parameter), it is important to relate this to the actual Eddington ratio (L_{bol}/L_{Edd}). To do so, we need a bolometric correction to the extinction corrected [OIII] luminosity. In Heckman et al. (2004) we showed that for Type 1 Seyfert nuclei and low-z quasars, the average bolometric correction to the *uncorrected* [OIII] luminosity was 3500. Typical measured values for the Balmer decrement in powerful AGN imply mean extinction corrections of ∼1.5 to 2 magnitudes (e.g Kewley et al. 2006), so we would expect the typical bolometric correction to the extinction corrected [OIII] luminosity for such AGN to be in the range ∼ 600 to 800. A more direct estimate comes from the combination of XMM X-ray, SDSS optical, and Spitzer mid-IR spectra of a complete flux-limited sample of SDSS Type 2 AGN (Heckman et al. in preparation). These data imply corresponding bolometric corrections in the range ∼500 to 800.

These values pertain to moderately powerful AGN with log L[OIII]/M$_{BH}$ > -0.5 (typically Type 2 Seyfert nuclei). The situation is less clear for the lower luminosity AGN (typically LINERs). First of all, the overall ionization state of the emission-line region is lower than in Seyfert nuclei, and so the [OIII] line will carry a smaller fraction of the total ionizing luminosity (Netzer 2009, in preparation). Second, the ratio of ionizing to total luminosity may be significantly different compared to the more powerful AGN (Ho 2008, but see Maoz 2007). We have therefore considered the low-luminosity AGN separately. Ho (2008) has derived a mean bolometric correction to the extinction-corrected Hα luminosity of ∼220 for low-luminosity AGN. Compared to the [OIII] line, the Hα emission-line suffers much more severe contamination from regions of star formation encompassed by the SDSS fiber (as quantified below). We have therefore converted the bolometric correction in Ho (2008) to the corresponding value for the [OIII] luminosity of ∼ 300 to 600. Since the ranges in the bolometric corrections for the lower- and higher-powered AGN overlap, for simplicity we will simply take a mean bolometric correction to the extinction-corrected [OIII] of 600. Thus, for $L/L_{Edd} = 1$, the corresponding value of log L[OIII]/M$_{BH}$ would be ∼1.7 dex.

In our past work, AGN have been identified according to their location in the Baldwin, Philipps & Terlevich (BPT; 1981) diagrams. In particular, in the space of [OIII]λ 5007/Hβ versus [NII]λ6583/Hα, AGN and star-forming galaxies are relatively well separated, with the AGN emerging as a plume from the bottom of the star-forming sequence, and extending upwards and outwards towards larger [OIII]/Hβ and [NII]/Hα values. Kauffmann et al. (2003b) used data from the SDSS to define a fiducial cut to separate star-forming galaxies from AGN. This is illustrated in Figure 1 where we plot BPT diagrams for four volume-limited samples of galaxies with $0.02 < z < 0.1$ divided according to black hole mass. We note that the SDSS spectra are measured using 3 arc second diameter fibres, which corresponds to a physical radii of $\sim 0.6 - 2.7$ kpc for the AGN in our sample (i.e. the spectra are mainly sampling the light from the bulges of the galaxies). In Figure 1, the dashed red curve shows our fiducial division between star-forming galaxies and AGN. AGN are plotted as red dots, while star-forming galaxies are plotted as black dots. We have included all the galaxies with $S/N > 3$ in each of the four emission lines used to define the BPT diagram.

There are two important points to note from Figure 1. First, there are a significant number of galaxies that lie near the boundary between star-forming galaxies and AGN, i.e. the separation

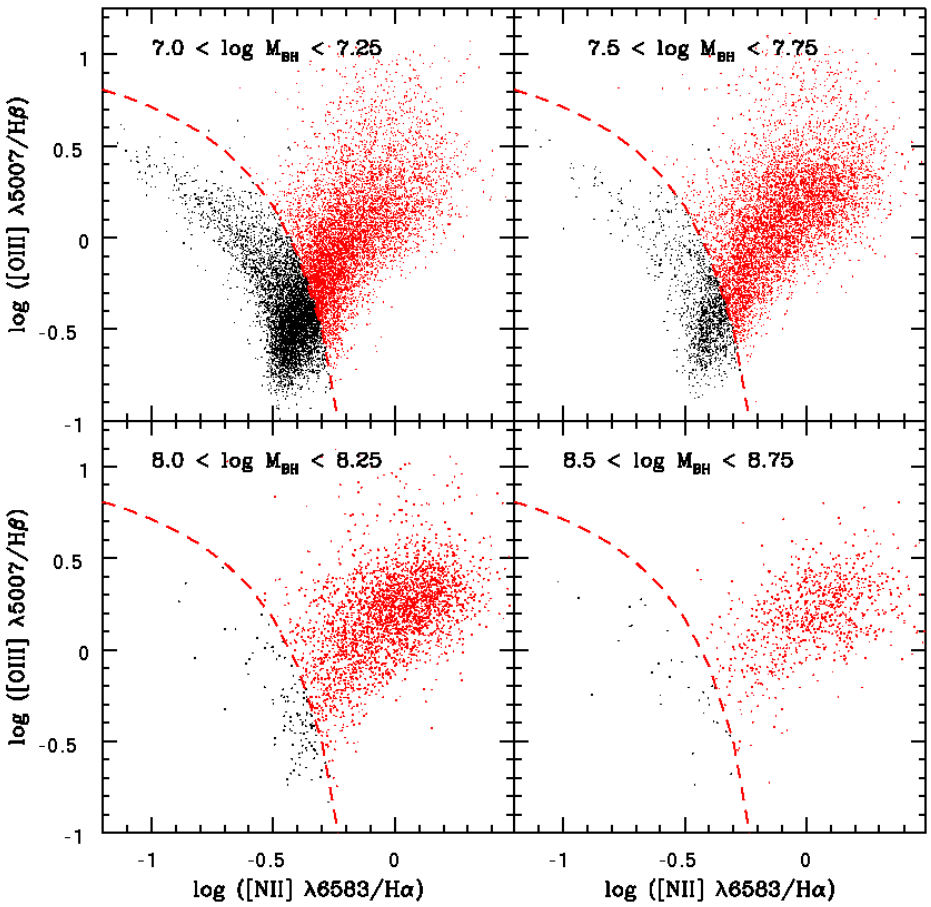

Figure 1: [OIII]λ 5007/Hβ versus [NII]λ6583/Hα BPT diagrams for a volume-limited sample of galaxies with $z < 0.1$. Only galaxies with $S/N > 3$ measurements of all four lines are shown. Results are shown in 4 different ranges of black hole mass. The dashed curve is the fiducial separation curve between star-forming galaxies and AGN defined in Kauffmann et al (2003b). Galaxies classified as AGN are plotted as red points, while galaxies classified as star-forming galaxies are plotted as black points.

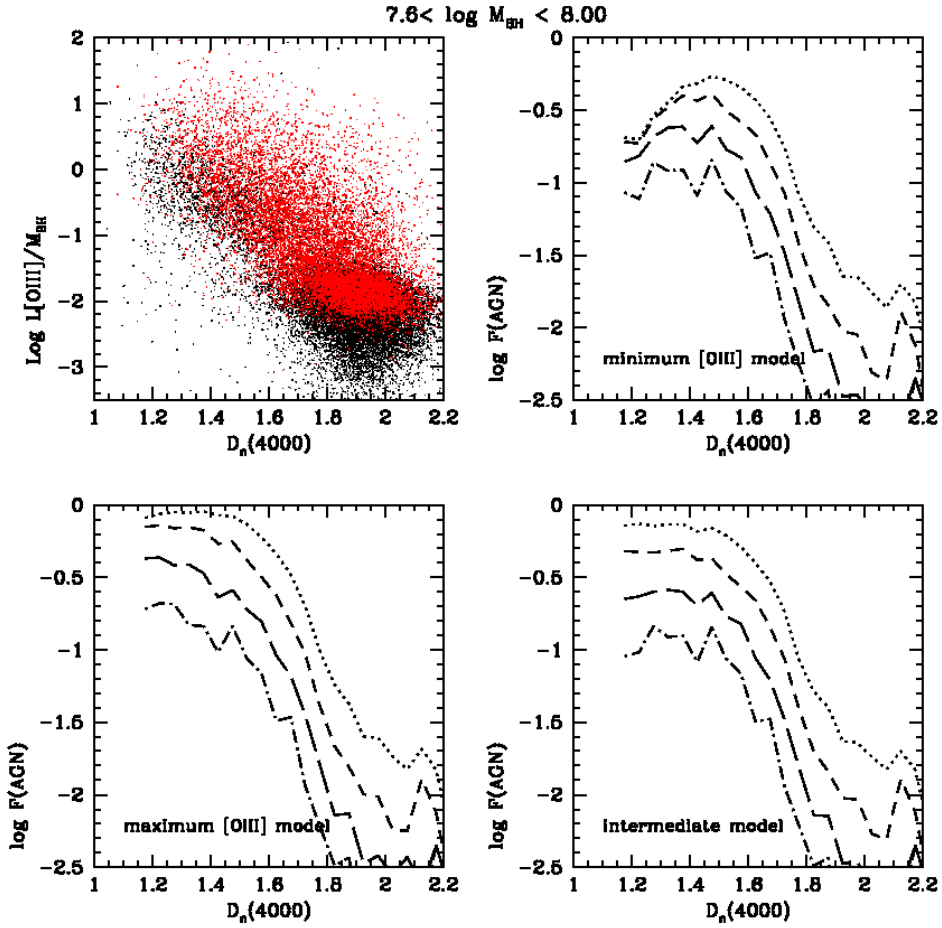

Figure 2: *Top left:* L[OIII]/M_{BH} is plotted as a function of 4000 Å break strength for a volume-limited sample of galaxies with $z < 0.1$ and black hole masses in the range $7.6 < \log M_{BH} < 8.0$. All galaxies are included in this diagram: if the [OIII] line is not detected, the upper limit in L[OIII]/M_{BH} is plotted. Black points denote star-forming galaxies or galaxies with emission lines that are too weak to classify. Red points denote AGN (the classification of AGN is the same as in Figure 1). *Top right:* The fraction of galaxies with L[OIII]/M_{BH} greater than a given value is plotted as a function of $D_n(4000)$. In this panel, L[OIII] is set to zero for all galaxies classified as star-forming on the BPT diagram. Dotted, short-dashed, long-dashed and dashed-dotted curves show results for L[OIII]/M_{BH} =-1.0, -0.5, 0.0 and 0.4, respectively. *Bottom left:* In this panel, L[OIII] is set to its measured value for galaxies classified as star-forming. *Bottom right:* In this panel, L[OIII] is set to one-third its measured value for galaxies classified as star-forming.

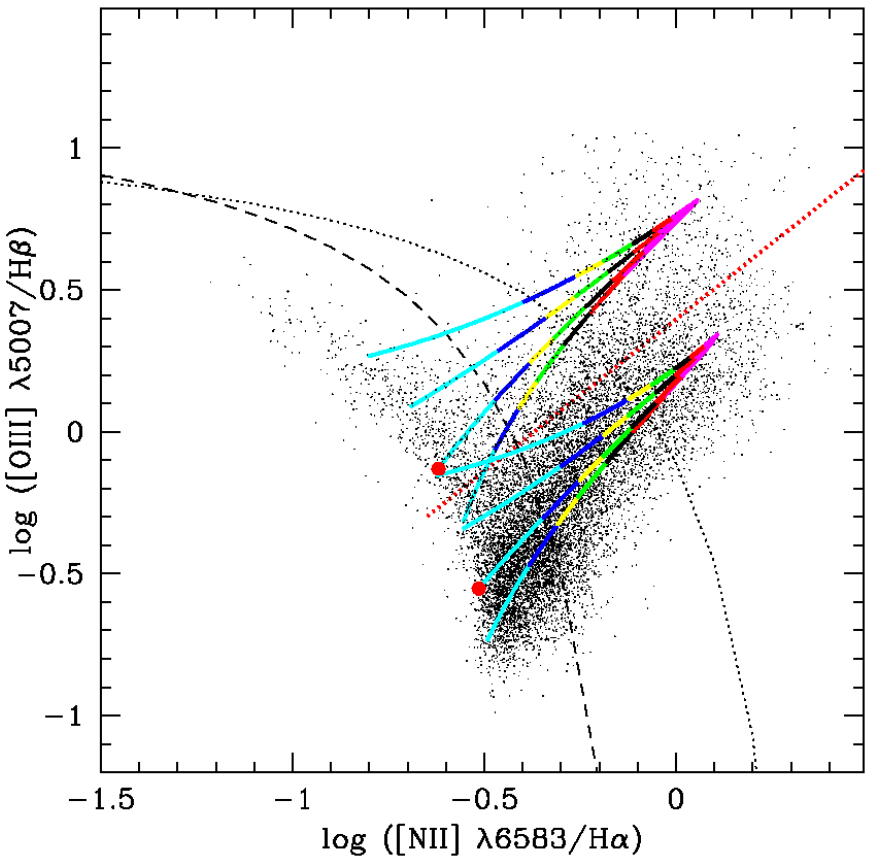

Figure 3: An illustration of star-forming/AGN mixing trajectories. Each curve shown on the plot connects a point on the star-forming locus to two possible "pure" AGN. The curves are coloured according to the fraction of the total [OIII] luminosity that originates from star formation. Cyan shows the part of the trajectory where the contribution from star formation is greater than a half, blue is where it is between 1/3 and 1/2, yellow between 1/4 and 1/3, green between 1/6 and 1/4, black between 1/6 and 1/9, red between 1/9 and 1/16 and magenta is where the SF contribution is less than 1/16th of the total [OIII] luminosity. The black dashed line shows the separation between star-forming galaxies and AGN defined by Kauffmann et al (2003b), while the black dotted line is the maximal starburst demarcation of Kewley et al (2001). The two red circles indicate the two trajectories that we use to correct the [OIII] luminosities of the galaxies in our sample, depending on whether they lie above or below the red dotted line (see text for more details).

between the two classes of objects is not a clean one. In fact, for the lower mass black holes (log $M_{BH} < 7.75$), the density of plotted points is actually constant or even rising as we approach the boundary and cross over from objects classified as AGN to those classified as star forming. This demonstrates that a sharp boundary dividing AGN and star forming galaxies is unphysical. The data simply define a continuum along which the relative contribution of the AGN and star-forming regions varies smoothly. Second, a larger fraction of galaxies with low mass black holes fall below our fiducial curve and are classified as star-forming galaxies. There are two reasons for this: 1) galaxies with low mass black holes have more ongoing star formation. For a fixed black hole accretion rate, the net ionizing radiation field will be softer, causing galaxies to fall closer to the star-forming locus, 2) galaxies with low mass black holes are smaller, so the 3 arc second fibre aperture will sample light than originates not only from the bulge of the galaxy, but also from the star-forming disk. Kauffmann et al (2003b) show that the age of the stellar population increases as a function of the distance of the AGN from the star-forming locus, which is consistent with both these hypotheses.

In Figure 2 (upper left) we plot our Eddington parameter, as a function of 4000 Å break strength, for a complete, volume-limited sample of galaxies with black hole masses in the range $10^{7.6}$ to $10^{8} M_{\odot}$. Galaxies classified as AGN are plotted as red points and galaxies classified as either star-forming galaxies or galaxies with undetected [OIII] emission-lines are plotted as black points (in the latter case the points are plotted at the value of the upper limit to the [OIII] luminosity).

This figure is useful to address two possible limitations of our data. The first is the fact that we will no longer be able to detect the [OIII] emission-line if it is too weak relative to the underlying stellar continuum. In fact, the abrupt disappearance of AGN below log L[OIII]/M_{BH} $\sim$ -2.5 for large values of $D_n(4000)$ simply reflects this limit. In the rest of the paper we will restrict our analysis to systems above this value. The second limitation has already been mentioned above (contamination of the emission-lines by star forming regions can mask the presence of an AGN). In this regard it is reassuring that we see in Figure 2 that for the younger bulges, the numbers of AGN simply decline smoothly towards low luminosities. In fact, there are rather few galaxies in the lower left quadrant of this figure. Thus, the decline in the number of AGN towards low luminosity in the younger bulges can not be produced by the misclassification of AGN as pure star forming galaxies.

While contamination by regions of star formation will not have a strong qualitative impact, it does pose a problem if we wish to derive a *complete* and accurate distribution function of Eddington ratios and understand how the distribution is modulated by how much star formation there is in the galaxy. That is, even in galaxies classified as star-forming, some fraction of the measured [OIII] line luminosity should probably be attributed to the AGN. We attempt to illustrate this in the next three panels of Figure 2, where we plot the fraction of all galaxies with Eddington parameter greater than some fixed value as a function of $D_n(4000)$. Dotted, short-dashed, long-dashed and dashed-dotted lines show results for increasing values of the Eddington parameter threshold (see caption). In the top right panel, we assume that *none* of the [OIII] luminosity in galaxies classified as star-forming should be attributed to the AGN. In this case, one sees that the fractions reach a peak value at $D_n(4000) \sim 1.5 - 1.6$. They drop steeply at higher values of $D_n(4000)$, but they also decline slightly at lower values. In the bottom left panel, we make the opposite assumption, i.e. *all* of the [OIII] luminosity in galaxies classified as star-forming show be attributed to the AGN. These two assumptions obviously bracket the full range of possibilities. What is interesting, is that even if we make the extreme assumption that all of the [OIII] should be attributed to the AGN, the AGN fraction dependence on $D_n(4000)$ is remarkably flat below a value of ~ 1.6. We will return to this point later. The bottom right panel shows an intermediate case in which a third of the [OIII] luminosity in the galaxies classified as star-forming actually comes from the AGN.

In the following analysis, we implement a simple method for partitioning the total [OIII] luminosity of a galaxy into the component from star formation and the component from the AGN,

based on the position of the galaxy on the BPT diagram. We assume that galaxies situated at the lower ridge of the star-forming sequence do not contain an AGN. We then create a set of pure star-forming galaxy templates at different positions along the star forming locus by averaging together the emission line luminosities of galaxies situated along this ridge. Likewise, we create two different "pure AGN" templates by averaging together the emission line luminosities of galaxies situated at the far end of the AGN sequence. We then create a set of mixing-line "trajectories" by averaging the emission line luminosities of the star-forming galaxy and AGN templates in different proportions.

These trajectories are illustrated in Figure 3. There are 8 curves shown on the plot, each connecting a point on the star-forming locus to two possible "pure" AGN. The curves are coloured according to the fraction of the total [OIII] luminosity that originates from star formation. Cyan shows the part of the trajectory where the contribution from star formation is greater than a half, blue is where it is between 1/3 and 1/2, yellow between 1/4 and 1/3, green between 1/6 and 1/4, black between 1/6 and 1/9, red between 1/9 and 1/16 and magenta is where the SF contribution is less than 1/16th of the total [OIII] luminosity. For galaxies at the boundary between the star-forming sequence and AGN as defined by Kauffmann et al. (2003b), the contribution to the [OIII] luminosity by star-formation is predicted to be typically 40 to 50%. By the time, the galaxy has crossed above the maximum-starburst curve defined by Kewley et al. (2001), the contribution to [OIII] from star formation has dropped to typically 10-20%. [1]

To simplify matters, we only use two of the trajectories in shown Figure 3 to estimate the fraction of the total [OIII] luminosity from star formation for each galaxy in our sample. One trajectory is representative of the population of lower ionization AGN (LINERs), and the other is a better match to higher ionization AGN (Seyferts). We calculate the distance to the upper red dot if the galaxy lies above the dotted red line, or to the lower red dot of the galaxy lies below this line. We then read off the correction to the [OIII] luminosity at the same distance along the trajectory linking the red dot to its corresponding pure AGN. The correction means that the fraction of the [OIII] luminosity contributed by star formation decreases smoothly with distance from the locus of pure star-forming galaxies in the BPT diagram. Although this procedure will not be accurate for individual galaxies, Figure 3 shows that it ought to work reasonably well for statistical analyses of the kind presented in this paper.

3 Eddington Ratio Distribution Functions

We now turn to an analysis of the distribution function of Eddington parameters. We note that our galaxies are drawn from the r-band selected Main spectroscopic sample with $14.5 < r < 17.77$ and in all our work, we are careful to weight by the appropriate $1/V_{max}$ factor to account for any luminosity-dependent selection effects that may be present.

In Figure 4, we begin by plotting the fraction of black holes with L[OIII]/M$_{BH}$ values above a given value (left panel). We also plot the fraction of the total [OIII] luminosity coming from such black holes (right). Cyan, blue, green. black, red and magenta curves indicate black holes of increasing mass, from 10^7 to $10^{8.25} M_{\odot}$ in steps of 0.25 dex in log M$_{BH}$. As discussed above, our adopted bolometric correction implies that an AGN with log L[OIII]/M$_{BH} \sim 1.7$ is accreting at about the Eddington rate. As seen in Figures 2 and 3, this value does indeed correspond to the upper limit of the Eddington parameters of the AGN in our sample.

[1] It is instructive to use the same sets of models to predict the fractional contribution by regions of star formation by other emission-lines in the SDSS spectra. For Hα, these values are 80-90% at the Kauffmann et al. (2003b) boundary and 50-60% at the Kewley et al. (2001) boundary. Values for the other strong emission-lines ([OII]3727, [NII]6584, and [SIII]6717,6731) are similar. The only line with similar behavior to [OIII]5007 is [OI]6300. However, this line is typically three to ten times weaker than the [OIII] line, and is therefore unable to probe the lowest luminosity AGN.

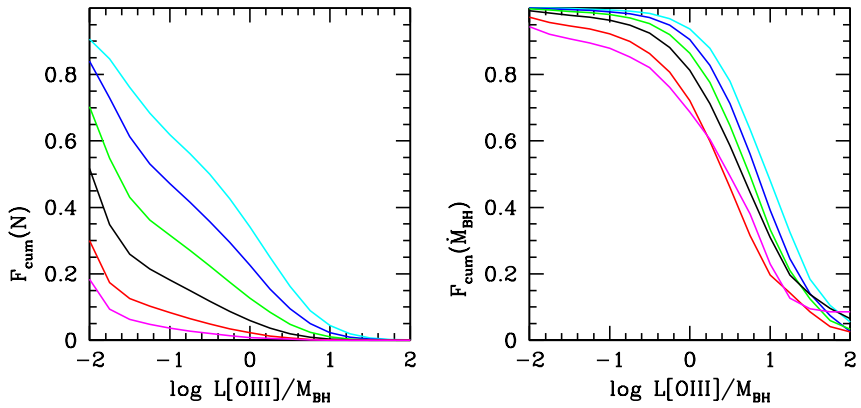

Figure 4: *Left:* The fraction of the total number of black holes with Eddington parameter L[OIII]/M_{BH} greater than a given value. *Right:* The fraction of the total mass accretion (as traced by the integrated [OIII] luminosity after correction for star formation) that is occurring in AGN with Eddington parameter L[OIII]/M_{BH} greater than a given value. Cyan, blue, green, black, red and magenta curves show results for black holes with log M_{BH} in the range (7.0-7.25; 7.25-7.5; 7.5-7.75; 7.75-8.0; 8.0-8.25; 8.25-8.5)

Figure 4 shows that the duty cycle of moderately powerful AGN activity in low mass black holes is quite high; more than 50% of all such black holes have log L[OIII]/$M_{BH} > -0.2$, corresponding to Eddington ratios of around 1 percent, and 90% have log L[OIII]/$M_{BH} > -2.2$. In higher mass black holes, the fraction of such moderate luminosity AGN decreases sharply and the population is dominated by systems that are accreting at less than 0.1 % Eddington. Nevertheless, the right-hand panel of Figure 4 shows that total black hole growth is always dominated by the most powerful AGN, irrespective of the black hole mass of the galaxy. Note that in order to calculate the total black hole growth, we integrate the [OIII] luminosities (corrected for star formation) of all galaxies with emission lines that are detected at high enough significance to allow them to be localized on the BPT diagram.

We now turn to an analysis of the differential Eddington ratio distribution function, i.e. the fraction of black holes of a given mass per unit logarithmic interval of λ=L[OIII]/M_{BH}. Figure 5 shows our derived Eddington parameter distribution functions in 6 different ranges of black hole mass. In this figure, one can clearly see the shift towards lower Eddington parameter as black hole mass increases. The distribution functions have quite complex shapes. For the lower mass black holes, there is a "bump" that is peaked at log [OIII]/M_{BH} of around 0.1 or so. For the higher mass black holes, the bump is barely discernible and the shape is closer to a power-law.

The origin of this complexity in shape becomes clear when we divide the galaxies in our sample into different bins in 4000 Å break strength. This is shown in Figure 6. The top panel shows Eddington parameter distribution function for all black holes in the range $10^7 - 10^8 M_{\odot}$. One can clearly see the bump at high values of log L[OIII]/M_{BH} and the power-law at low values of log L[OIII]/M_{BH}. In the two bottom panels, we divide the galaxies into different bins in $D_n(4000)$ and the plot the distribution functions for these different subsamples. The left panel shows the results for 5 subsamples with $D_n(4000) < 1.5$. It is remarkable that the distribution functions are nearly independent of $D_n(4000)$ over this range and are well-characterized by a log-normal function. The right panel shows results for 5 subsamples with $D_n(4000) > 1.5$. In this regime, the distribution function depends strongly on $D_n(4000)$: the fraction of high L[OIII]/M_{BH} objects decreases for

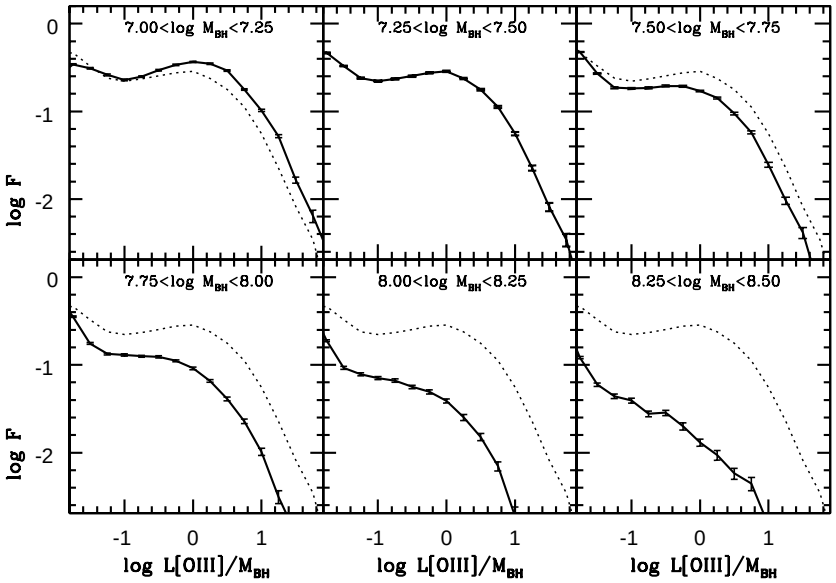

Figure 5: The logarithm of the fraction of black holes of a given mass per unit logarithmic interval in λ=L[OIII]/M$_{BH}$ is plotted as a function of log L[OIII]/M$_{BH}$, for six ranges of black hole mass. The dotted line in each panel shows the result for black holes in the mass range $7.25 < \log M_{BH} < 7.50$.

larger values of D$_n$(4000) and the shape tends increasingly towards a power-law.

In Figure 7, we explore how these results depend on the mass of the black hole. We have chosen two representative ranges in 4000 Å break strength: 1.2 <D$_n$(4000)< 1.4, corresponding to "young" galaxies, and 1.7 <D$_n$(4000)< 1.9, corresponding to "old" galaxies. We plot the distribution functions of our Eddington ratio parameter for different ranges of black hole mass. We see that the log-normal distribution is not only independent of the precise value of 4000 Å break strength for galaxies with D$_n$(4000)< 1.5 (Figure 6), it is also independent of black hole mass. The best fit log-normal function is centered at a value of log L[OIII]/M$_{BH}$=0.1 and has a dispersion of 0.4 dex. As shown in the right panel, however, the slope of the power-law is roughly constant (~ -0.7) for different mass black holes, but there is a dependence in the amplitude – Eddington ratios are apparently lower for galaxies with more massive black holes.

Although it is clear from Figure 7 that the shape of the accretion rate distribution functions are quite distinct in galaxies with "young" and "old" stellar populations, it is important to note that *the accretion rate distribution is very broad in both populations.* Indeed, in galaxies with black hole masses less than a few $\times 10^7 M_\odot$, the fraction of systems that are accreting near Eddington differs rather little between the two populations. The main distinguishing characteristic is that for the young population, the distribution peaks at a characteristic value of about 2.5 percent Eddington [2] , but this peak is not present for galaxies with old stellar populations. This means that the likelihood for the black holes in young galaxies to be accreting at rates very close to Eddington is small , but so is the probability for such black holes to be accreting at very low rates or not to be accreting at

[2]We note that the precise position of the peak is sensitive to how we choose to correct the [OIII] luminosities of the galaxies in our sample for star formation. For example, if we simply assign a third of the [OIII] luminosity of all galaxies lying below the Kauffmann et al (2003b) demarcation curve to the AGN, and 100% of the [OIII] luminosity from galaxies above this curve to the AGN, we obtain a broader distribution peaked at 0.5 percent Eddington. However, the bell-like shape of the distribution function and our conclusion that it peaks at values much less than Eddington is robust. It holds even if if we assign 100% of the [OIII] luminosity in all galaxies to the AGN.

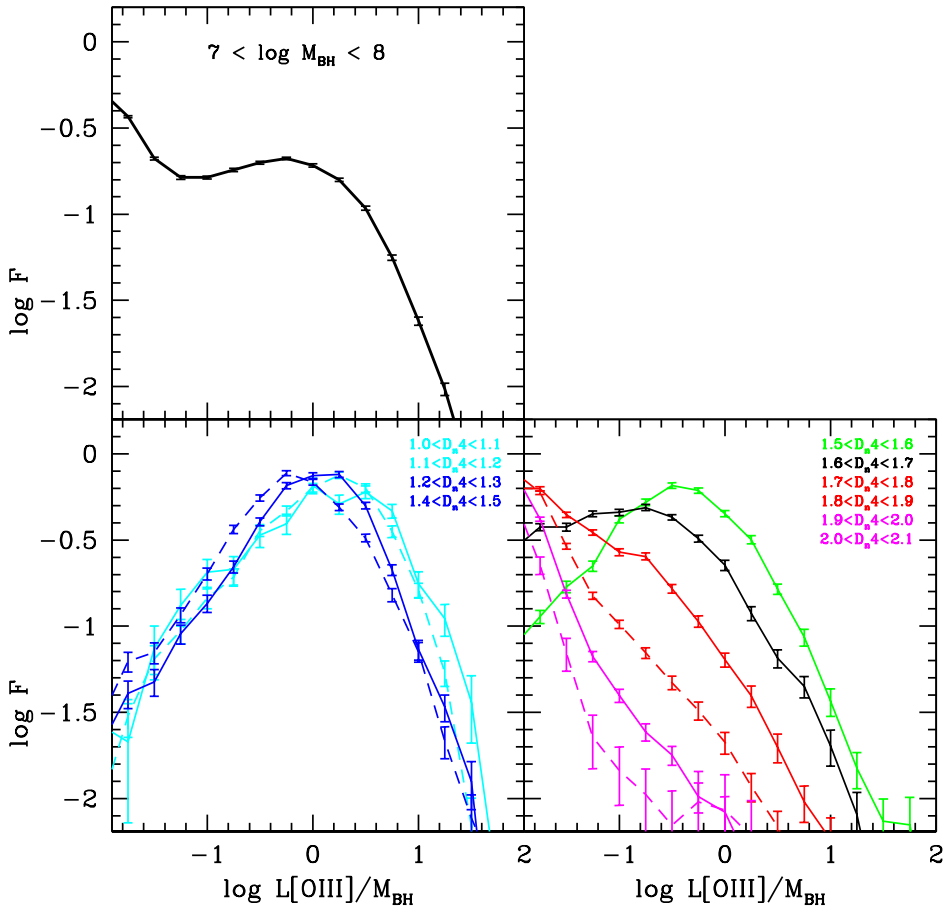

Figure 6: *Top:* The logarithm of the fraction of black holes per unit logarithmic interval in λ=L[OIII]/M$_{BH}$, and with masses in the range $10^7 - 10^8 M_\odot$ and is plotted as a function of log L[OIII]/M$_{BH}$. *Bottom:* The accretion rate distributions of subsamples split into different ranges in 4000 Å break strength as indicated.

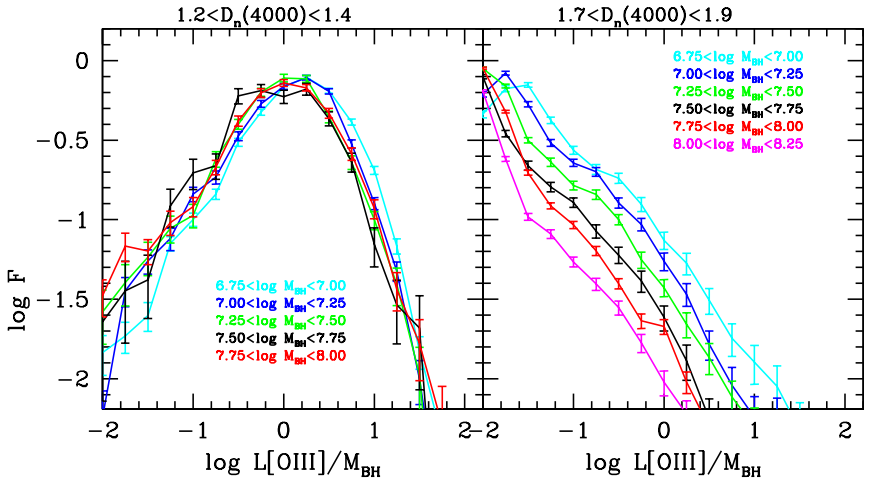

Figure 7: The logarithm of the fraction of black holes per unit logarithmic interval in λ=L[OIII]/M$_{BH}$, with masses in the range $10^7 - 10^8 M_\odot$ a is plotted as a function of log L[OIII]/M$_{BH}$ for different ranges of black hole mass. The left panel shows results for young galaxies with 1.2 <D$_n$(4000)< 1.4 and the right panel shows results for old galaxies with 1.7 <D$_n$(4000)< 1.9 (right). The Eddington parameter distribution in the left panel is well-fit with a log-normal function centred at log L[OIII]/M$_{BH}$=0.1 and with a dispersion of $\sim$ 0.4 dex. In the right panel, the distribution can be characterized as a power-law with slope $\sim -0.6 - -0.8$.

all. On the other hand, black holes in galaxies with old stellar populations spend most of their time inactive or accreting at very low rates, but accretion near the Eddington luminosity is still possible under certain (rare) conditions. This point is again apparent in Figure 8, where we show plots of the cumulative fraction of the total mass accretion onto black holes that is occurring above a given value of the Eddington parameter, in six different ranges of 4000 Å break strength. The different coloured lines show results for different ranges of black hole mass. We see that over most of the range in black hole mass and stellar age, the growth of black holes is dominated by the most actively growing systems (50% of the growth is occurring in systems accreting at greater than 5 to 10% of the Eddington limit). However, for the biggest black holes in the oldest bulges, this median value drops to only 0.1 to 1% Eddington.

Finally, Figure 9 shows the fraction of the total mass accretion occurring in the "log-normal" (defined as D$_n$(4000)< 1.7) versus the "power-law" (defined as D$_n$(4000)> 1.7) regimes as a function of black hole mass. For low mass black holes, $\sim$ 80% of the accretion is occuring in the log-normal mode. This fraction decreases for more massive black holes – the two modes of black hole growth become roughly equal for black holes of $\sim 10^8 M_\odot$. At larger black hole masses, the "power-law" mode dominates. Integrating over black holes of all masses, we find that 76% of the total mass accretion in the local Universe is occuring in the log-normal regime at the present day. Thus, both modes of black hole growth are significant.

4 Towards a Physical Understanding of these Results

Our basic result is that we have uncovered two regimes of black hole growth in the local Universe. One regime is associated with galaxies with D$_n$(4000) < 1.5 (galaxies with significant recent/on-going star formation) and is characterized by a log-normal distribution function of accretion rates

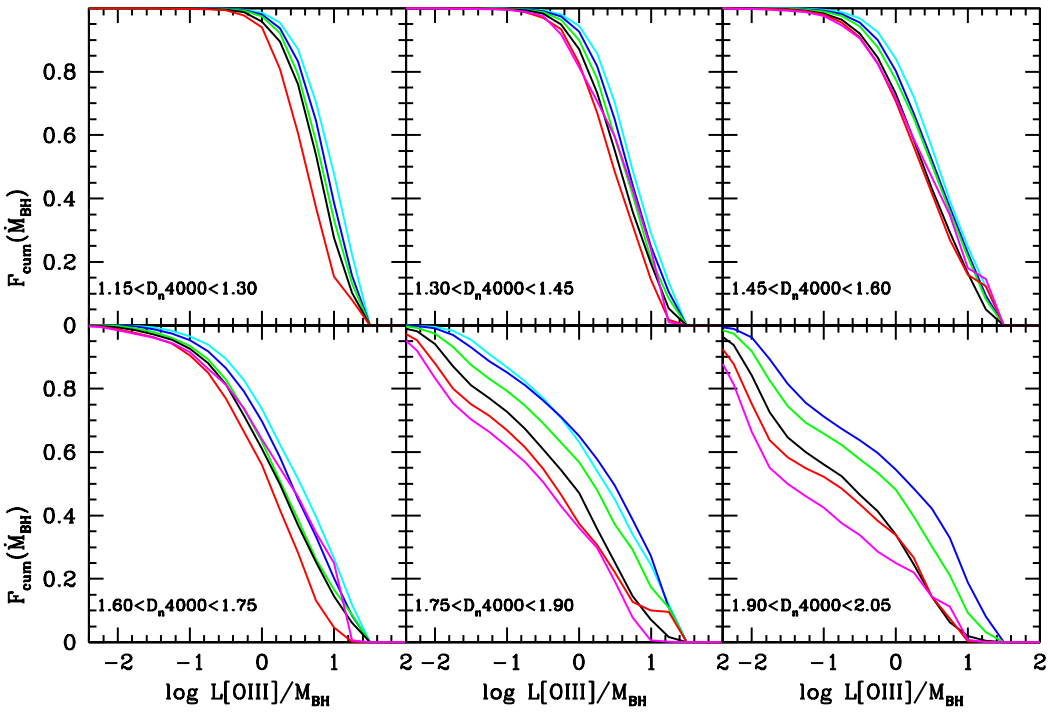

Figure 8: The fraction of the total mass accretion (as traced by the integrated [OIII] luminosity) that is occurring in AGN with Eddington parameter L[OIII]/M$_{BH}$ greater than a given value. Different panels are for subsamples in different ranges of 4000 Å break strength. Cyan, blue, green, black, red and magenta curves show results for black holes with log M_{BH} in the range (7.0-7.25; 7.25-7.5; 7.5-7.75; 7.75-8.0; 8.0-8.25; 8.25-8.5)

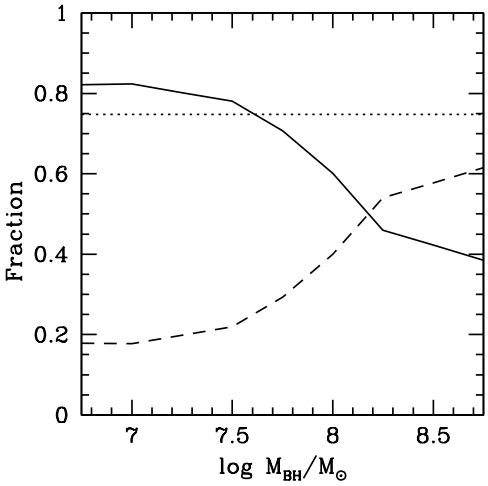

Figure 9: The fraction of the total mass accretion (as traced by the integrated [OIII] luminosity) that is occurring in the "log-normal" mode (solid line) and the "power-law" mode (dashed line) as a function of black hole mass. The dotted line shows the fraction of the total mass accretion onto all black hole that is occurring the log-normal mode.

that is peaked at value of $L[OIII]/M_{BH}$ corresponding to a few percent of the Eddington rate. The other regime is associated with galaxies with $D_n(4000) > 1.8$ (little or no star formation) and is characterized by a power-law-like distribution function of accretion rates, extending down to the detection threshold of the [OIII] line in our SDSS spectra.

4.1 The log-normal regime

Our most striking conclusion about the log-normal regime is that the accretion rate distribution function remains largely invariant if we adopt different cuts on galaxy properties. It is independent of the velocity dispersion of the stars in the bulge and by extension, it is independent of the mass of the black hole. It is also at most weakly dependent on the fraction of young stars measured within the SDSS fibre aperture, which implies that the accretion onto the black hole is insensitive to the properties of the interstellar medium as measured inside radii of ~ 1 kpc.

Thus in the log-normal regime, accretion onto the black hole is apparently not limited by the supply of gas, but by feedback processes that are intrinsic to the black hole itself, such as winds from the accretion disk (Begelman, McKee & Shields 1983; Murray et al 1995) or small-scale radio jets (Ulvestad & Wilson 1989; Kellerman et al 1998). One could imagine a situation where the black hole flares to a luminosity near Eddington when it first accretes some gas and this is followed by a period of latency, because feedback processes disrupt the gas supply in the vicinity of the black hole. Indeed, the location of the peak of the distribution at a few percent of Eddington may reflect an accretion rate threshold where the feedback starts to become important. It has been pointed out by many authors that radiative feedback effects are predicted to reduce steady state accretion onto the black hole to $\sim 1\%$ Eddington (e.g. Ostriker et al. 1976, Proga et al 2008, Milosavljevic et al 2008). This main difference between our picture and that envisgaed by Hopkins & Hernquist (2008) is that the feedback is not strong enough to disrupt and expel the entire interstellar medium of the galaxy. If this was the case, one would not obtain a log-normal distribution of accretion rates, with a decrease in the fraction of objects accreting at low luminosities relative to those accreting

at intermediate luminosities. In low redshift AGN the bulk of the gas in the bulge remains intact, and after a period of time that is short compared to the age of the Universe, gas will again begin to accrete onto the black hole.

These results help us understand why no clear connection has been established between the presence of central bars or dust lanes and the fueling of AGN in local galaxies (e.g. Martini et al. 2003). If the effect of feedback from the black hole is limited only to the gas very near the black hole, and if the AGN lifetime is relatively brief, then we would not expect to see systematic differences in the kpc-scale properties of young bulges with and without a strong AGN. These results also help us understand why there is no connection between mergers/interactions and black hole accretion rate in AGN in the local Universe. Galaxy-galaxy interactions drive gas from the outer disk into the central kiloparsec of the galaxy, where it can fuel a starburst. Indeed, we do see strong signatures of this process in the SDSS data (Li et al 2008; Reichard et al 2008). However, this increase in gas supply has no significant impact on the accretion onto the central black hole for reasons that we have discussed above.

4.2 The power-law regime

At first sight, the power-law regime appears more complicated. Figures 6 and 7 show that the amplitude of the power law appears to depend on both black hole mass and on $D_n(4000)$. However, in Figure 10, we show that the picture simplifies considerably if we plot distribution functions of the quantity L[OIII]/M(bulge), where M(bulge) is the dynamical mass of the galaxy bulge, which we estimate using the formula M(bulge)= $(1.65\sigma)^2 R_{50}/G$, where R_{50} is the half-light radius of the galaxy (see Padmanabhan et al 2004). Figure 10 shows that the slope of the power-law ($\sim$ -0.8) is similar to before, but now the distributions are no longer dependent on black hole mass and only scale with $D_n(4000)$.

This implies that in the power-law regime, the total accretion onto the black hole is simply proportional to the stellar mass in the bulge, with a constant of proportionality that scales with the mean stellar age of the stars in the bulge. The simplest interpretation of this result is that black holes in this regime are being fueled by stellar mass loss.

Norman & Scoville (1988) discussed a model in which stellar mass loss from an evolving nuclear starburst fueled the growth of a central super-massive black hole. They found that the evolution of the stellar mass-loss over the range from 100 Myr to 10 Gyr after the burst could be parameterized as a power-law in time with a slope in the range -1.1 to -1.5 (leading to the same scaling for the luminosity of the accreting black hole). Following Hogg & Phinney (1997), the resulting slope of the luminosity function $dN/dlnL$ for this population would be in the range -0.7 to -0.9. This is in excellent agreement with our measured slope for power-law distribution of the Eddington ratio.

We can further test our model by using standard population synthesis models (Bruzual & Charlot 2003; Maraston 2005) to predict how mass loss rates ought to scale as a function of $D_n(4000)$, and to investigate whether this agrees with the change in the average value of L[OIII]/M_* as a function of $D_n(4000)$ for the AGN in our sample. This is shown in Figure 11. The dots show the predicted mass loss rate (in units of the fraction of the stellar mass returned per Gigayear) as a function of $D_n(4000)$ for galaxies with different star formation histories. We parametrize these histories using a range of formation times, exponential decline time scales and burst probabilities as described in Kauffmann et al (2003a). Black dots show results using mass loss rates taken from Bruzual & Charlot (2003), while magenta dots are for Maraston (2005). A Kroupa (2001) IMF is assumed in both cases. The coloured curves show how the average value of L[OIII]/M(bulge) changes as a function of $D_n(4000)$ for galaxies with black holes in different mass ranges. As can be seen, the predicted mass loss rates decrease by a factor of ~ 3 as $D_n(4000)$ goes from a value of 1.6 to a value of 2.1. The corresponding

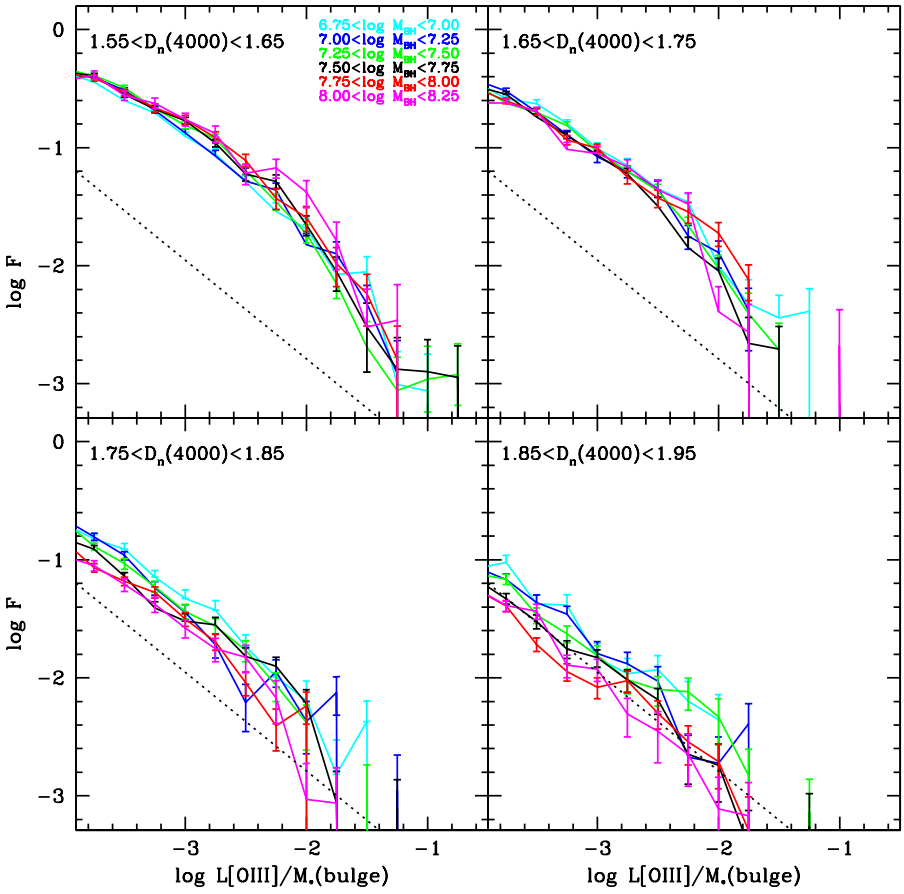

Figure 10: The distribution function of the ratio of the [OIII] line luminosity to bulge dynamical mass for galaxies split by black hole mass and by 4000 Å break strength. We plot the fraction of black holes per unit logarithmic interval in log L[OIII]/M(bulge). The 4 different panels show results for four different ranges in 4000 Å break strength, Cyan, blue, green, black, red and magenta curves show results for black holes with log M_{BH} in the range (7.0-7.25; 7.25-7.5; 7.5-7.75; 7.75-8.0; 8.0-8.25; 8.25-8.5). The dotted black line shows a power-law with a slope of -0.8 adjusted to pass through the data in the lower right panel.

drop in L[OIII]/M$_*$ is somewhat larger, but taking into account the uncertainties in the IMF in the dense inner regions of galaxy bulges (Maness et al 2007), the fact that the two quantities scale to within a factor of two is encouraging.

We have also tried scaling the [OIII] luminosities by the stellar mass of the whole galaxy and we find L[OIII]/M$_*$ distributions functions that are still independent of black hole mass, but with somewhat more scatter. It is important to recall that our analysis always deals with average accretion rates, and not accretion rates for individual AGN. Because we are considering accretion rates averaged over a large population of objects, it is not unreasonable to suppose that if the main source of fuel is mass loss from evolved stars, the average accretion rate will scale with the stellar mass of the galaxy bulge. On the other hand, if one were able to "zoom in" very close to the active nucleus, then the *instantaneous* accretion rate onto the black hole and the mass and mean age of the stars in the *immediate vicinity* of the nucleus may correlate with much less scatter. Recently, Davies et al (2007) have analyzed star formation in the nuclei of nine Seyfert galaxies at spatial resolutions

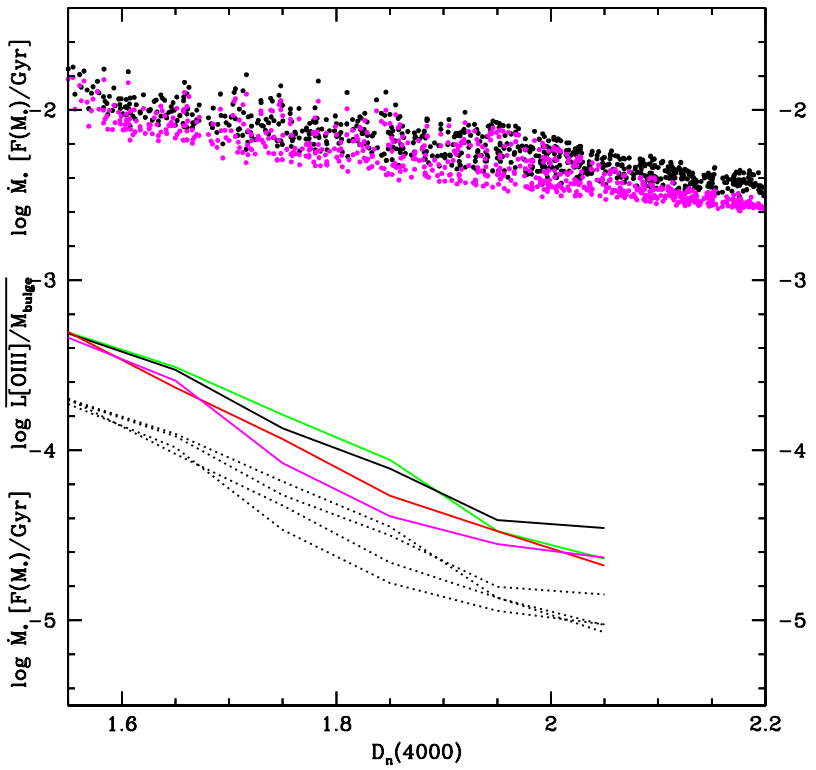

Figure 11: The black dots show the mass loss rate per Gyr normalized to the stellar mass predicted by BC03 models (black) and Maraston (2005) models (magenta) as a function of $D_n(4000)$ for a variety of exponentially declining star formation histories. The coloured curves show the mean value of L[OIII]$/M(bulge)$ (in units of solar luminosities per solar mass). as a function of $D_n(4000)$ for galaxies with older stellar populations. Green, black, red and magenta curves show results for black holes with log M_{BH} in the range (7.25-7.5; 7.5-7.75; 7.75-8.0; 8.0-8.25). The dotted black curves show the implied mass accretion rate onto the black hole per Gyr (again normalized to the stellar mass), if we assume a bolometric correction factor $L_{bol}/L_{[OIII]} \sim 600$ and a radiative efficiency of 10%. The ratio of the normalized accretion rates for these dotted curves to those of the models (black and magenta points) indicates the fraction of the stellar mass loss that would need to be accreted by the black hole. The implied ratios are ~ 0.3 to 1%.

corresponding to length scales of around 10 pc. They find evidence for young stars in the near vicinity of all the nuclei, but in many of the systems, star formation has already terminated. These results suggest a scenario in which nuclear star formation occurs in multiple short bursts, as gas (perhaps originating from the material shed by stars further out in the bulge) flows into the central regions of the galaxy. Interestingly, the luminosity of the AGN appears to be *positively* correlated with the age of the starburst, peaking at ages of 100-300 Myr. It is then argued that this may imply that winds from AGB stars, which have low velocities, may supply the gas which actually flows onto the central black hole. This time delay agrees with the prediction of Norman & Scoville (1988).

Finally, we use our fiducial bolometric correction factor L_{bol}/L[OIII]$\sim$ 600, plus an assumed radiative efficiency of 10%, to transform the average L[OIII]/M_* values into estimates of the average black hole accretion rate. This is shown as the set of dotted curves at the bottom of the plot (again, per Gyr normalized to the stellar mass of the bulge). The ratio of this accretion rate to the mass-loss rate predicted by the models yields the fraction of the mass-loss from the stellar bulge that must be accreted by the black hole to produce the observed line radiation. Figure 11 then implies that this fraction is between 0.3-1%. This is in good agreement with Ciotti & Ostriker (2007), who model how AGN activity is triggered by recycled gas from evolved stars. These models predict that half the gas from dying stars is ejected as galactic winds, half is consumed in central starbursts and less than 1% is accreted onto the central black hole. The Norman & Scoville (1988) model assumed much higher accretion efficiency, although their source of the mass-loss was a compact (10 pc-scale) nuclear star cluster, and they did not consider feedback from the black-hole.

5 Final Thoughts & Conclusions

As we have shown, the changeover from AGN in the log-normal regime to AGN in the power-law regime starts to occur at a 4000 Å break strength of $\sim$ 1.5 and is complete by values above $\sim$1.8. We can use the calibration of $D_n(4000)$ in terms of the star formation rate per unit mass in Brinchmann et al. (2004) to examine the physical significance of these values. We use Figure 11 in Brinchmann et al., but consider the inverse quantity: M_*/SFR (i.e. the characteristic timescale for growing the bulge due to star formation). This figure then shows that over the range in $D_n(4000)$ spanned by the log-normal regime, this growth time increases from about 5 Gyr (for $D_n(4000) = 1.2$) to about 20 Gyr (for $D_n(4000) = 1.5$). In other words, the log-normal regime corresponds to galaxy bulges that are growing significantly today (M_*/SFR $\sim$ the Hubble time). This figure also shows that in the pure power-law regime ($D_n(4000) > 1.8$), the growth time is about two orders-of-magnitude longer than the Hubble time (i.e. these are dead systems). Finally, the intermediate regime of $D_n(4000) = 1.5$ to 1.8 where AGN transition from the pure log-normal to pure power-law regime corresponds to a similar transition between systems with short and very long growth times (from $\sim$ 20 to 1000 Gyr). In simple terms, the behavior of the distribution of the Eddington parameter implies that the log-normal and power-law regimes correspond almost exactly to the populations of "living" and "dead" galaxy bulges.

In conclusion, therefore, optical emission lines trace two distinct modes of black hole growth in the present-day universe. We have shown that these two modes are strongly linked to the formation history of the stellar population of the bulges that host the black holes. These links provide important clues as to how black holes are fueled and how this fueling may regulate their further growth.

One mode is associated with galaxy bulges that are undergoing significant star-formation. More quantitatively, these are bulges in which the present stellar mass can be formed at the current star-formation rate on a timescale of-order the Hubble time. Thus, these are systems in which the build up of the stellar population has taken place gradually over the history of the universe. For these black holes, the distribution of the Eddington-ratio (L/L_{Edd}) takes a log-normal form that is

universal with respect to both the mass of the black hole and the current star formation rate. This regime dominates the growth of black holes with masses less than $\sim 10^8$ $M_\odot$. As shown by Heckman et al. (2004), the mass-doubling time for this population of black holes is of-order a Hubble time.

The other mode is associated with galaxy bulges with little or no on-going star-formation. In these systems, the formation of the stars in the bulge occurred long ago. For this population of black holes, the distribution of the Eddington-ratio is a power-law with a universal slope, but with a normalization that depends on the age of the stellar population. We have shown that the slope and age-dependence of the normalization are predicted by a simple model in which the black hole accretes on-average ~ 0.3 to 1% of the mass lost by evolved bulge stars. This regime dominates the growth of the more massive black holes ($> 10^8$ $M_\odot$), the population with an insignificant present-day growth rate (Heckman et al. 2004).

As has been discussed by many authors, the galaxy population is the local Universe is also strongly bimodal in nature, with galaxies separating into two clearly defined "peaks", both in terms of their structure and their stellar populations (Strateva et al 2002; Kauffmann et al 2003c; Baldry et al 2004). This has led to considerable speculation as to the physical mechanisms that are responsible for creating the two distinct populations. One idea is that feedback from the AGN may be powerful enough to expel much of the interstellar medium of the galaxy, causing star formation to shut down over short time scales and the galaxy to transit from the blue to the red population. We have argued that the log-normal Eddington ratio distribution functions for galaxies with young bulges are inconsistent with catastrophic feedback from the black hole that operates on the scale of the whole galaxy (or even of the bulge). Instead, it is likely that the log-normal distribution of the Eddington ratio is set by a long-running competition between the sporadic supply of cold gas from the bulge to the black hole and subsequent feedback that operates locally (speculatively, within the sphere of influence of the black hole $r < GM_{BH}/\sigma^2_{bulge}$). Once the gas runs out, black hole growth appears to be regulated by the rate at which evolved stars lose their mass. The picture of black hole growth that appears to emerge from our results is thus very much a "passive" one.

One question one might ask is whether the low redshift AGN studied in this paper are fundamentally different in nature to quasars at higher redshifts. Kollmeier et al (2006) concluded that in higher redshift quasars, the distribution of estimated Eddington ratios is also well described as log-normal, but with a peak at much higher luminosities ($L_{\rm bol}/L_{\rm Edd} = 1/4$). As pointed out in a number of papers (e.g. Netzer et al 2007, Gavignaud et al 2008, Hopkins et al 2009), selection effects imply only objects with uniformly high accretion rates will be optically identified as quasars. Only when we have complete samples of *galaxies* selected by bulge or black hole mass where the energetic output of the central black holes can be characterized down to reasonably low levels, will we be able to make a fair comparison between low and high redshift samples.

For the moment, we believe that the origin of the bimodal nature of the galaxy population still remains as a major unsolved problem. Given the continued cosmological infall of gas, why is the only fuel available to black holes in massive galaxies material shed by old stars? At least at low-redshifts, it is likely that radio AGN play an active role in suppressing the cooling of gas in the dark matter halo, keeping such systems in the power-law "slow starvation" regime (Best et al. 2005, 2007). It remains to be seen whether the same picture will still hold up at higher redshifts.

Acknowledgments

We thank Philip Hopkins, Reinhard Genzel, Colin Norman, Jerry Ostriker, Simon White and Francesco Shankar for useful conversations that inspired this work.

Funding for the SDSS and SDSS-II has been provided by the Alfred P. Sloan Foundation, the Participating Institutions, the National Science Foundation, the U.S. Department of Energy, the National

Aeronautics and Space Administration, the Japanese Monbukagakusho, the Max Planck Society, and the Higher Education Funding Council for England. The SDSS Web Site is http://www.sdss.org/.

The SDSS is managed by the Astrophysical Research Consortium for the Participating Institutions. The Participating Institutions are the American Museum of Natural History, Astrophysical Institute Potsdam, University of Basel, University of Cambridge, Case Western Reserve University, University of Chicago, Drexel University, Fermilab, the Institute for Advanced Study, the Japan Participation Group, Johns Hopkins University, the Joint Institute for Nuclear Astrophysics, the Kavli Institute for Particle Astrophysics and Cosmology, the Korean Scientist Group, the Chinese Academy of Sciences (LAMOST), Los Alamos National Laboratory, the Max-Planck-Institute for Astronomy (MPIA), the Max-Planck-Institute for Astrophysics (MPA), New Mexico State University, Ohio State University, University of Pittsburgh, University of Portsmouth, Princeton University, the United States Naval Observatory, and the University of Washington.

References

Adelman-McCarthy J. K., et al., 2006, ApJS, 162, 38

Baldry I. K., Glazebrook K., Brinkmann J., Ivezić Ž., Lupton R. H., Nichol R. C., Szalay A. S., 2004, ApJ, 600, 681

Baldwin J. A., Phillips M. M., Terlevich R., 1981, PASP, 93, 5

Balogh, M.L., Morris, S.L., Yee, H.K.C., Carlberg, R.G., Ellingson, E., 1999, ApJ, 527, 54

Barnes J. E., Hernquist L. E., 1991, ApJ, 370, L65

Barnes J. E., Hernquist L., 1996, ApJ, 471, 115

Begelman M. C., McKee C. F., Shields G. A., 1983, ApJ, 271, 70

Best P. N., Kauffmann G., Heckman T. M., Ivezić Ž., 2005, MNRAS, 362, 9 (B05b)

Best P. N., von der Linden A., Kauffmann G., Heckman T. M., Kaiser C. R., 2007, MNRAS, 379, 894

Brinchmann J., Charlot S., White S. D. M., Tremonti C., Kauffmann G., Heckman T., Brinkmann J., 2004, MNRAS, 351, 1151

Bruzual G., Charlot S., 2003, MNRAS, 344, 1000

Cid Fernandes R., Gu Q., Melnick J., Terlevich E., Terlevich R., Kunth D., Rodrigues Lacerda R., Joguet B., 2004, MNRAS, 355, 273

Ciotti L., Ostriker J. P., 1997, ApJ, 487, L105

Ciotti L., Ostriker J. P., 2007, ApJ, 665, 1038

Croton D. J., et al., 2006, MNRAS, 365, 11

Davies R. I., Mueller Sánchez F., Genzel R., Tacconi L. J., Hicks E. K. S., Friedrich S., Sternberg A., 2007, ApJ, 671, 1388

Di Matteo T., Springel V., Hernquist L., 2005, Nature, 433, 604

García-Burillo S., Combes F., Schinnerer E., Boone F., Hunt L. K., 2005, A&A, 441, 1011

Gavignaud, I. et al, 2008, A&A, 492, 637

Granato G. L., De Zotti G., Silva L., Bressan A., Danese L., 2004, ApJ, 600, 580

Hao L., et al., 2005, AJ, 129, 1783

Heckman T. M., Kauffmann G., Brinchmann J., Charlot S., Tremonti C., White S. D. M., 2004, ApJ, 613, 109

Ho L. C., Filippenko A. V., Sargent W. L. W., 1997, ApJS, 112, 315

Ho L. C., 2008, ARA&A, 46, 475

Hogg, D. W., Phinney, E. S., 1997, ApJ, 488, L95

Hopkins P. F., Hernquist L., Cox, T.J., Di Matteo T., Martini P., Robertson, B., Springel, V., 2005a, ApJ, 630, 705

Hopkins P. F., Hernquist L., Martini P., Cox T. J., Robertson B., Di Matteo T., Springel V., 2005b, ApJ, 625, L71

Hopkins P. F., Hernquist L., 2008, arXiv, arXiv:0809.3789

Hopkins, P.F., Hickox, R., Quataert, E., Hernquist, L. 2009, arXiv:0901.2936

Kauffmann G., Haehnelt M., 2000, MNRAS, 311, 576

Kauffmann G., et al., 2003a, MNRAS, 341, 33

Kauffmann G., et al., 2003b, MNRAS, 346, 1055

Kauffmann G., et al., 2003c, MNRAS, 341, 33

Kellermann K. I., Vermeulen R. C., Zensus J. A., Cohen M. H., 1998, AJ, 115, 1295

Kewley L. J., Dopita M. A., Sutherland R. S., Heisler C. A., Trevena J., 2001, ApJ, 556, 121

Kewley L. J., Geller M. J., Jansen R. A., Dopita M. A., 2002, AJ, 124, 3135

Kewley L. J., Groves B., Kauffmann G., Heckman T., 2006, MNRAS, 372, 961

Kollmeier J. A., et al., 2006, ApJ, 648, 128

Kroupa, P., 2001, MNRAS, 322, 231

Li C., Kauffmann G., Wang L., White S. D. M., Heckman T. M., Jing Y. P., 2006, MNRAS, 373, 457

Li C., Kauffmann G., Heckman T. M., White S. D. M., Jing Y. P., 2008, MNRAS, 385, 1915

Maness H., et al., 2007, ApJ, 669, 1024

Maoz, D., 2007, MNRAS, 377, 1696

Maraston C., 2005, MNRAS, 362, 799

Martini P., Weinberg D. H., 2001, ApJ, 547, 12

Martini P., Regan M. W., Mulchaey J. S., Pogge R. W., 2003, ApJ, 589, 774

Mathews W. G., Baker J. C., 1971, ApJ, 170, 241

Mihos J. C., Hernquist L., 1996, ApJ, 464, 641

Milosavljevic, M., Couch, S.M., Bromm, V., 2008, eprint arXiv:0812.2516

Murray N., Chiang J., Grossman S. A., Voit G. M., 1995, ApJ, 451, 498

Netzer, H., Lira, P., Trakhtenbrot, B., Shemmer, O., Cury, Iara, 2007, ApJ, 671, 1256

Norman, C., Scoville, N., 1988, ApJ, 332, 124

Ostriker, J., Weaver, R., Yahil, A., McCray, R., 1976, ApJ, 208, L61

Padmanabhan N., et al., 2004, NewA, 9, 329

Proga, D., Ostriker, J., Kurosawa, R., 2008, ApJ, 676, 101

Reichard T. A., Heckman T. M., Rudnick G., Brinchmann J., Kauffmann G., Wild V., 2008, arXiv, arXiv:0809.3310

Sanders D. B., Soifer B. T., Elias J. H., Madore B. F., Matthews K., Neugebauer G., Scoville N. Z., 1988, ApJ, 325, 74

Shankar F., Crocce M., Miralda-Escude' J., Fosalba P., Weinberg D. H., 2008, arXiv, arXiv:0810.4919

Shen Y., et al., 2007, AJ, 133, 2222

Shlosman I., Frank J., Begelman M. C., 1989, Natur, 338, 45

Soltan A., 1982, MNRAS, 200, 115

Springel V., Di Matteo T., Hernquist L., 2005, MNRAS, 361, 776

Strateva I., et al., 2001, AJ, 122, 1861

Tremaine S., et al., 2002, ApJ, 574, 740

Ulvestad J. S., Wilson A. S., 1989, ApJ, 343, 659

York D. G., et al., 2000, AJ, 120, 1579

Yu Q., Tremaine S., 2002, MNRAS, 335, 965